JOC*Article*

A Computational Study of Oxiranyllithium

Lawrence M. Pratt*

Department of Chemistry, Fisk University, 1000 17th Avenue North, Nashville, Tennessee 37208

B. Ramachandran

Chemistry, College of Engineering & Science, Louisiana Tech University, Ruston, Louisiana 71272

lpratt@fisk.edu

Received May 3, 2005

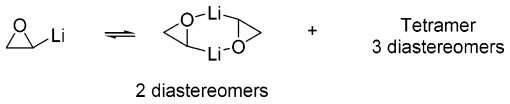

Computational methods were used to determine the structure, bonding, and aggregation states of oxiranyllithium in the gas phase and in THF solution, at 200 and 298 K. THF solvation was modeled by microsolvation with explicit THF ligands, forming a supermolecule that includes the oxiranyllithium aggregate and its first solvation shell. Because oxiranyllithium has a chiral center, two diastereomeric dimers were formed, the *RR* and the *RS*, along with their enantiomers. Similarly, three diastereomers of the tetramer were formed, the *RRRR*, *RRRS*, and *RRSS* and their enantiomers. Oxiranyllithium was found to exist predominantly as the tetramer in the gas phase, while the dimer was the dominant species in THF solution. The relative concentrations of the different stereoisomers were calculated from equilibrium constants.

Introduction

Oxiranyllithium compounds have attracted attention in recent years as important synthetic intermediates. As a kind of α-lithioether, they could potentially behave as either a lithium carbenoid or a chelated alkyllithium. Lithiation of a carbon adjacent to an oxygen atom is usually unfavorable unless the product is stabilized by conjugation or electron-withdrawing groups. Thus, experimental data on simple α-lithioethers is sparse. Cyclic ethers are more readily lithiated, but the resulting lithioethers rapidly decompose, and the properties of those species are deduced from their reaction products. The most common reactions of oxiranyllithiums are with electrophiles, similar to those of alkyllithiums.[1−7] Carbenoid-like reactions of oxiranyllithiums have also been reported, and the carbenoid character of these compounds has been investigated by isotopic labeling and kinetic studies.[8−11] From these studies, it appears that oxiranyllithium compounds may be intermediate in properties between lithium carbenoids and chelated alkyllithiums. The purpose of this study is to more fully determine the structure, bonding, and aggregation state of oxiranyllithium by computational methods, in hopes of better understanding its properties and reactions.

Because of the instability of simple, unstabilized oxiranyllithiums, we turned to computational methods to investigate their properties, including bonding and aggregation state. Hartree−Fock and DFT methods have been previously used to study the monomer of some oxiranyllithiums that were stabilized by chelating functional groups.[1,7] In this work, oxiranyllithium was modeled in the gas phase to determine its structure without the influence of coordinating solvent ligands and in THF solution. The solution-phase calculations were modeled by a microsolvation model in which the inner solvent sphere is represented by explicit THF ligands. This model

(1) Alickmann, D.; Frohlich, R.; Wurthwein, E.-U. *Org. Lett*. **2001**, *3*, 1527.
(2) Capriati, V.; Florio, S.; Luisi, R.; Nuzzo, I. *J. Org. Chem.* **2004**, *69*, 3330.
(3) Hodgson, D. M.; Reynolds, N. J.; Coote, S. J. *Org. Lett*. **2004**, *6*, 4187.
(4) Luisi, R.; Capriati, V.; Degennaro, L.; Florio, S. *Org. Lett.* **2003**, *5*, 2723.
(5) Mori, Y.; Nogami, K.; Hayashi, H.; Noyori, R. *J. Org. Chem*. **2003**, *68*, 9050.
(6) Capriati, V.; Degennaro, L.; Favia, R.; Florio, S.; Luisi, R. *Org. Lett*. **2002**, *4*, 1551.
(7) Abbotto, A.; Capriati, V.; Degennaro, L.; Florio, S.; Luisi, R.; Pierrot, M.; Salomone, A. *J. Org. Chem*. **2001**, *66*, 3049.
(8) Morgan, K. M.; Gajewski, J. J. *J. Org. Chem*. **1996**, *61*, 820.
(9) Hodgson, D. M.; Fleming, M. J.; Stanway, S. J. *J. Am. Chem. Soc*. **2004**, *126*, 12250.
(10) Wiedemann, S. H.; Ramirez, A.; Collum, D. B. *J. Am. Chem. Soc*. **2003**, *125*, 15893.
(11) Satoh, T. *Chem. Rev*. **1996**, *96*, 3303.

10.1021/jo050887n CCC: $30.25
Published on Web 08/11/2005

has proven successful for several other studies of organolithium compounds.[12−16]

Computational Methods

All calculations were performed using Gaussian 98 or Gaussian 03.[17] The gas-phase and solution energies reported include gas-phase internal energy, thermal corrections to the free energy at 200 and 298 K, and where applicable, solvation terms.

The solvation free energy change of the gas-phase organolithium molecule $(RLi)_n$ due to microsolvation by m explicit ethereal solvent ligands E (in this case, THF) is calculated by considering the process

$$(RLi)_n + mE \rightarrow (RLi)_n mE \quad (1)$$

The microsolvation model assumes that the free energy change accompanying this reaction adequately represents the solvation free energy ΔG°_{solv} of the solute $(RLi)_n$ in the solvent E, so that

$$G^\circ_T\,(\text{solute}) = G^\circ_T\,(\text{gas}) + \Delta G^\circ_{solv} \quad (2)$$

In other words, the free energy of a "supermolecule" $(RLi)_n mE$ relative to that of m solvent molecules is assumed to yield the free energy of the solvated molecule $(RLi)_n$ in the condensed phase. The gas-phase free energies of the relevant species are obtained computationally as

$$G^\circ_T\,(\text{gas}) = E_{en} + \Delta G^\circ_T \quad (3)$$

where the terms on the right-hand side as well as the procedure used for calculating them are described below. The geometry of each molecule was first optimized using the B3LYP hybrid density functional method[18,19] with the MIDI! basis set.[20] A further refinement of the geometry and energy was done at the B3LYP/6-31+G(d)[21,22] level of theory. Thus, we have

E_{en} = the electronic energy plus nuclear repulsion of the equilibrium geometry, using B3LYP/6-31+G(d)

E_0^{vib} = unscaled B3LYP/MIDI! vibrational zero-point energy

ΔG°_T = B3LYP/MIDI! thermal corrections to the free energy for a standard state of 1 atm and specified temperature from the masses. This includes contributions from translational, rotational, and vibrational degrees of freedom

Calculations for the free energy changes for the "reactions" (dimerizations, tetramerizations, etc.) are straightforward using the G°_T(gas) terms defined in eq 3.

The standard state of a solution is taken as 1 mol L^{-1}, and an additional correction to the free energy terms is needed to convert the standard state of an ideal gas (1 atm) to the standard state of the solution. This was incorporated by simply adding the term $RT\ \ln(RT)$ to each free energy term, where the numerical value of the argument of the logarithm was obtained using the pressure−volume (0.082057 L atm K^{-1} mol^{-1}) value for the gas constant. These corrections amount to 1.1120 kcal/mol at 200 K and 1.8943 kcal/mol at 298 K. These correction terms were included in all solution phase reactions below, i.e., calculations where the microsolvation model was used.

Yet another correction is required for proper treatment of the explicit solvent molecules used in microsolvation. The traditional approach is to set the standard state of a pure liquid to be the concentration of the pure liquid itself, which then allows one to drop the concentration of the pure liquid from equilibria expressions (consider the ionic product of water, for example). However, since we have decided to adopt the standard state of 1 mol L^{-1} for all species, the free energy change for the process

$$2\ RLi{\cdot}2THF \rightarrow (RLi{\cdot}THF)_2 + 2THF \quad (4)$$

is given by[23]

$$\Delta G^\circ = -RT \ln \frac{[(RLi{\cdot}THF)_2]}{[RLi{\cdot}2THF]^2} - 2\,RT \ln [THF] \quad (5)$$

The molarity of the THF solvent was calculated to be 13.26 at 200 K, and 12.33 at 298 K, from its tabulated density.[24] The corrections due to the second term in the equation above amount to −1.0273 and −1.4883 kcal/mol per THF at 200 and 298 K, respectively.

Basis set superposition errors may be significant when calculating dimerization and tetramerization energies of alkyllithiums because the higher aggregates contain more basis functions than the monomers. Counterpoise calculations are used to correct for these errors.[25] Because the solvated dimerization and tetramerization reactions are not isodesmic, direct calculation of the BSSE's is difficult. However, it is expected that the BSSE for each aggregate will be similar in the solvated and unsolvated forms. Therefore, the BSSE was calculated for each gas-phase monomer and tetramer, and that value was added to both the gas-phase and microsolvated aggregates.

Results and Discussion

The optimized geometry of the gas-phase oxiranyllithium monomer is shown in Figure 1. Chelation of the

(12) Pratt, L. M. *Bull. Chem. Soc. Jpn.* **2005**, *78*, 890.
(13) Pratt, L. M.; Mu, R.; Jones, D. *J. Org. Chem.* **2005**, *70*, 101.
(14) Pratt, L. M.; Mu, R. *J. Org. Chem.* **2004**, *69*, 7519.
(15) Pratt, L. M.; Mogali, S.; Glinton, K. *J. Org. Chem.* **2003**, *68*, 6484.
(16) Pratt, L. M.; Newman, A.; St. Cyr, J.; Johnson, H.; Miles, B.; Lattier, A.; Austin, E.; Henderson, S.; Hershey, B.; Lin, M.; Balamraju, Y.; Sammonds, L.; Cheramie, J.; Karnes, J.; Hymel, E.; Woodford, B.; Carter, C. *J. Org. Chem.* **2003**, *68*, 6387.
(17) Frisch, M. J.; Trucks, G. W.; Schlegel, H. B.; Scuseria, G. E.; Robb, M. A.; Cheeseman, J. R.; Montgomery, J. A., Jr.; Vreven, T.; Kudin, K. N.; Burant, J. C.; Millam, J. M.; Iyengar, S. S.; Tomasi, J.; Barone. V.; Mennucci, B.; Cossi, M.; Scalmani, G.; Rega, N.; Petersson, G. A.; Nakatsuji, H.; Hada, M.; Ehara, M.; Toyota, K.; Fukuda, R.; Hasegawa, J.; Ishida, M.; Nakajima, T.; Honda, Y.; Kitao, O.; Nakai, H.; Klene, M.; Li, X.; Knox, J. E.; Hratchian, H. P.; Cross, J. B.; Adamo, C.; Jaramillo, J.; Gomperts, R.; Stratmann, R. E.; Yazyev, O.; Austin, A. J.; Cammi, R.; Pomelli, C.; Ochterski, J. W.; Ayala, P. Y.; Morokuma, K.; Voth, G. A.; Salvador, P.; Dannenberg, J. J.; Zakrzewski, V. G.; Dapprich, S.; Daniels, A. D.; Strain, M. C.; Farkas, O.; Malick, D. K.; Rabuck, A. D.; Raghavachari, K.; Foresman, J. B.; Ortiz, J. V.; Cui, Q.; Baboul, A. G.; Clifford, S.; Cioslowski, J.; Stefanov, B. B.; Liu, G.; Liashenko, A.; Piskortz, P.; Komaromi, I.; Martin, R. L.; Fox, D. J.; Keith, T.; Al-Laham, M. A.; Peng, C. Y.; Nanayakkara, A.; Challacombe, M.; Gill, P. M. W.; Johnson, B.; Chem, W.; Wong, M. W.; Gonzalez, C.; Pople, J. A. *Gaussian 03, Revision A.1*; Gaussian, Inc.: Pittsburgh, PA, 2003.
(18) Becke, A. D. *J. Chem. Phys.* **1993**, *98*, 5648.
(19) Stephens, P. J.; Devlin, F. J.; Chabalowski, G. C.; Frisch, M. J. *J. Phys. Chem.* **1994**, *98*, 11623.
(20) Thompson, J. D.; Winget, P.; Truhlar, D. G. *Phys. Chem. Commun.* **2001**, *16*, 1.
(21) Lynch, B. J.; Zhao, Y.; Truhlar, D. G. *J. Phys. Chem.* **2003**, *107*, 1384.
(22) Clark, T.; Chandresekhar, J.; Schleyer, P. v. R. *J. Comput. Chem.* **1983**, *4*, 294.
(23) Thompson, J. D.; Cramer, C. J.; Truhlar, D. G. *J. Chem. Phys.* **2003**, *119*, 1661.
(24) Govender, U. P.; Letcher, T. M.; Garg, S. K.; Ahluwalia, J. C. *J. Chem. Egn. Data* **1996**, *41*, 147.
(25) Simon, S.; Duran, M.; Dannenberg, J. J. *J. Chem. Phys.* **1996**, *105*, 110214.

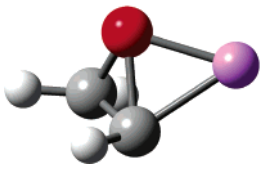

FIGURE 1. Optimized geometry of the oxiranyllithium monomer: gray, carbon; white, hydrogen; red, oxygen; violet, lithium.

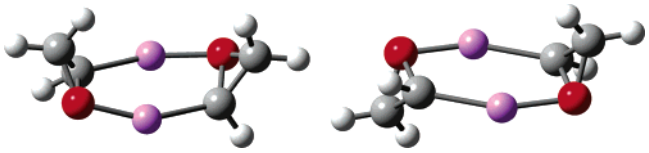

FIGURE 2. Optimized geometry of the oxiranyllithium dimers: left, *RR* isomer; right, *RS* isomer.

TABLE 1. Gas-Phase Dimerization Free Energies of Oxiranyllithium (kcal/mol)

	200 K		298 K	
isomer	BSSE uncorrected	BSSE corrected	BSSE uncorrected	BSSE corrected
RR	−42.1	−39.9	−38.4	−36.1
RS	−42.2	−39.9	−38.5	−36.2

lithium atom by oxygen caused the geometry of the carbon atom to distort from the structure of oxirane, the H−C_α−Li angle in the monomer being 132° as opposed to the H−C−H angle of 115.5° found in oxirane. The distortion is also evident in the 60.5° dihedral angle H−C_β−C_α−Li compared to the H−C_β−C_α−H of 0° in oxirane. Similar distortion of bond angles in tetravalent carbon atoms has been reported for lithiocarbenoids.[26,27]

In contrast to the monomer, the bonding in the gas-phase oxiranyllithium dimer resembles that in oxirane, with the lithium atoms replacing the hydrogens. Two diastereomeric dimers were formed, the *RR* and the *RS*, as shown in Figure 2, together with their enantiomers. The gas-phase dimerization free energies, calculated according to eq 6, are given in Table 1. The two diastereomers were essentially equally stable, with a slight energetic preference for the *RS* isomer. Higher temperatures reduced the tendency of oxiranyllithium to dimerize by a few kcal/mol. Basis set superposition errors (BSSE) were more than two kcal/mol, as determined by counterpoise calculations on the dimers at the B3LYP/6-31+G(d) level.

$$2(\text{oxiranyllithium monomer}) \rightarrow \text{dimer} \qquad (6)$$

The optimized geometry of the gas-phase oxiranyllithium tetramer is shown in Figure 3. The geometry of the *RRRR* diastereomer resembled that of alkyllithium tetramers, with the lithium-bearing carbon atoms at the face of a tetrahedron of lithium atoms. In the case of oxiranyllithium, these lithium atoms were also chelated by the oxygen atoms. The geometries of the *RRRS* and *RRSS* diastereomers were similar, but with more distortion of the tetrahedra of lithium atoms. The data in Table 2, calculated by eq 7, show the calculated free energy of tetramer formation from the monomer. The *RRRS* diastereomer was slightly more stable than the other two isomers. As with the dimer, counterpoise calculations showed significant BSSEs at the B3LYP/6-31+G(d) level. To determine whether the dimer or the tetramer is the predominant species in the gas phase, the free energy of tetramer formation from the most stable *RS* dimer was calculated according to eq 8. The results are shown in Table 3 and show that the tetramer predominates in the gas phase at both 200 K and at 298 K.

TABLE 2. Gas-Phase Tetramerization Free Energies of Oxiranyllithium (kcal/mol)

	200 K		298 K	
isomer	BSSE uncorrected	BSSE corrected	BSSE uncorrected	BSSE corrected
RRRR	−98.6	−91.6	−86.1	−79.2
RRRS	−99.3	−91.7	−87.1	−79.5
RRSS	−97.1	−90.3	−85.5	−78.7

TABLE 3. Gas-Phase Free Energies of Oxiranyllithium Tetramer Formation from the Dimer (kcal/mol)

	200 K		298 K	
isomer	BSSE uncorrected	BSSE corrected	BSSE uncorrected	BSSE corrected
RRRR	−14.1	−11.8	−9.11	−6.83
RRRS	−14.8	−11.9	−10.1	−7.18
RRSS	−12.6	−10.4	−8.47	−6.26

TABLE 4. Calculated Free Energies of Tetrasolvated Dimer Formation from the Disolvate (kcal/mol)

isomer	$\Delta G^\circ_{200\ K}$	$\Delta G^\circ_{298\ K}$
RR	−0.255	5.44
RS	−0.768	4.51

$$4(\text{oxiranyllithium monomer}) \rightarrow \text{tetramer} \qquad (7)$$

$$2(\text{oxiranyllithium } RS \text{ dimer}) \rightarrow \text{tetramer} \qquad (8)$$

Microsolvation by THF ligands generated structures similar to those in the gas phase. The optimized geometry of the oxiranyllithium monomer is shown in Figure 4. Like the gas-phase structure, the solvated monomer showed significant carbenoid-like distortion of the tetravalent carbon bond angles, as well as lithium chelation by the epoxide oxygen atom.

The THF-solvated dimers also exhibited similar bonding to the gas-phase structures, as shown in Figure 5. Geometry optimizations were performed on both the disolvated and tetrasolvated dimers, and the results are shown in Table 4, according to eq 9. The calculations showed a slight preference for the tetrasolvated form at 200 K and that the disolvated form predominates at 298 K. Therefore, the disolvated form was used in all subsequent calculations. Unlike the monomer, the carbon−lithium bonds had a geometry similar to those in oxirane. The dimerization energies, given in Table 5, indicate that oxiranyllithium is aggregated in THF solution, although the dimerization energy is less exergonic than in the gas phase. In contrast to the gas phase, the *RR* diastereomer was favored over the *RS* by nearly 2 kcal/mol. The BSSE

(26) Pratt, L. M.; Ramachandran, B.; Xidos, J. D.; Cramer, C. J.; Truhlar, D. G. *J. Org. Chem.* **2002**, *67*, 7607.
(27) Pratt, L. M.; Ngan, N. V.; Le, L. T. *J. Org. Chem.* **2005**, *70*, 2294.

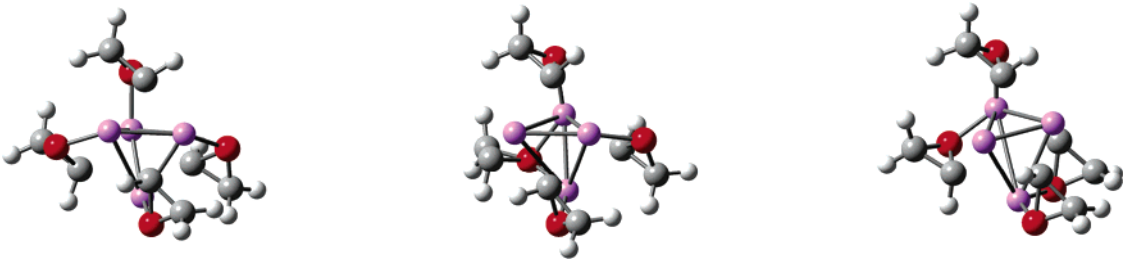

FIGURE 3. Optimized geometry of the oxiranyllithium tetramers: left, *RRRR* isomer; middle, *RRRS* isomer; right, *RRSS* isomer.

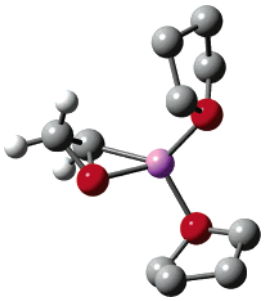

FIGURE 4. Optimized geometry of the THF disolvated oxiranyllithium monomer.

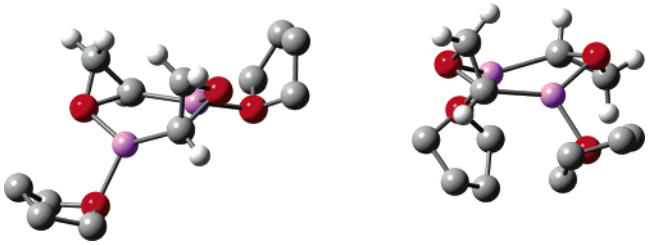

FIGURE 5. Optimized geometries of the THF disolvated oxiranyllithium dimers: left, *RR*; right, *RS*.

TABLE 5. Dimerization Free Energies of THF Disolvated Oxiranyllithium (kcal/mol)

	200 K		298 K	
isomer	BSSE uncorrected	BSSE corrected	BSSE uncorrected	BSSE corrected
RR	−14.2	−12.0	−17.1	−14.9
RS	−12.4	−10.1	−14.8	−12.5

corrections for the solvated dimerization reaction were assumed to be similar to those of the gas-phase dimerization, and the gas-phase values were used to calculate the energies in Table 5.

$$\text{dimer·2THF} + 2\text{THF} \rightarrow \text{dimer·4THF} \qquad (9)$$

The THF solvated tetramers also optimized to distorted tetrahedral structures, similar to those in the gas phase (Figure 6). The *RRRS* and *RRSS* structures were particularly distorted from the tetrahedral geometry by coordination of oxirane oxygen atoms to more than one lithium atom. The tetramerization energies are given in Table 6 for the process

$$4\text{RLi·2THF} \rightarrow (\text{RLi·THF})_4 + 4\text{THF} \qquad (10)$$

As in the gas phase, the three tetramer diastereomers were similar in energy. Although tetramer formation from the monomer is exergonic even in THF, the data in Table 7 show that the solvated tetramers would dissociate into disolvated dimers under standard conditions. Comparing Tables 3 and 7, we therefore conclude that oxiranyllithium is primarily tetrameric in the gas phase and dimeric in THF solution.

TABLE 6. Tetramerization Free Energies of THF-Disolvated Oxiranyllithium (kcal/mol)

	200 K		298 K	
isomer	BSSE uncorrected	BSSE corrected	BSSE uncorrected	BSSE corrected
RRRR	−25.8	−18.9	−26.3	−19.4
RRRS	−25.2	−17.6	−25.5	−17.9
RRSS	−26.9	−20.0	−27.3	−20.4

TABLE 7. Free Energies of THF-Solvated Oxiranyllithium Tetramer Formation from the Dimer (kcal/mol)

	200 K		298 K	
isomer	BSSE uncorrected	BSSE corrected	BSSE uncorrected	BSSE corrected
RRRR	2.59	4.67	7.84	9.92
RRRS	3.19	5.94	8.63	11.4
RRSS	1.41	3.42	6.78	8.79

TABLE 8. Relative Concentrations (in mol L^{-1}) of Dimeric and Tetrameric Species in the Gas Phase, Resulting from a Total 1.0 mol L^{-1} of Li (in Whatever Form)

isomer	200 K	298.15 K
RR	1.09×10^{-7}	7.43×10^{-4}
RS	1.40×10^{-7}	1.31×10^{-3}
RRRR	0.093	0.054
RRRS	0.154	0.175
RRSS	2.75×10^{-3}	0.020

The concentrations of the different species present at equilibrium from a total initial Li concentration were estimated from the equilibrium constants. It was assumed that a total of 1.0 mol L^{-1} of Li (in whatever form) is available. In the gas phase, because of the large, negative, free energy change for dimerization, it was assumed that the monomer concentration at equilibrium was essentially zero. Only the BSSE corrected free-energy changes from Table 3 were used to calculate equilibrium constants. The results are reported in Table 8.

Similar calculations were also performed for the solution-phase equilibria. However, since the $\Delta G°$ for dimerization (Table 5) are considerably smaller than that in the gas phase (Table 1), the monomer concentration at equilibrium was explicitly calculated. Only the disolvated

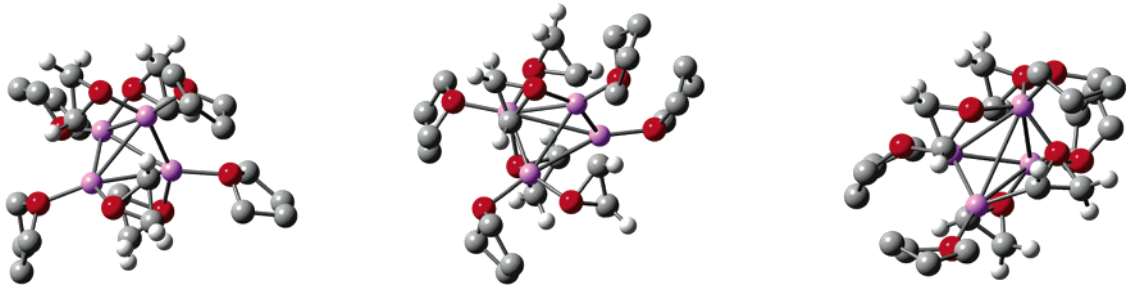

FIGURE 6. Optimized geometries of the THF tetrasolvated oxiranyllithium tetramers: left, *RRRR*; center, *RRRS*; right, *RRSS*.

TABLE 9. Relative Concentrations (in mol L^{-1}) of Dimeric and Tetrameric Species in THF Solution, Resulting from a Total 1.0 mol L^{-1} of Li (in Whatever Form)

species	200 K	298 K
R	2.59×10^{-6}	2.99×10^{-6}
RR	0.496	0.491
RS	4.16×10^{-3}	8.56×10^{-3}
RRRR	1.94×10^{-6}	1.29×10^{-8}
RRRS	6.66×10^{-10}	1.85×10^{-11}
RRSS	4.50×10^{-5}	8.71×10^{-8}

dimers were considered in these calculations. The results are reported in Table 9. The details of these calculations are available in the Supporting Information.

As stated in the Introduction, the nature of the carbons in the lithiated oxirane molecule is of considerable interest. Since Mulliken charges are often contrary to chemical intuition and experimental electronegativities, we obtained electrostatic surface potential (ESP) fitted charges using the Merz−Singh−Kollman algorithm.[28] The use of ESP-derived charges has been well-validated in other work.[29] In the neutral oxirane molecule, partial negative charges are assigned to both carbons (−0.16 on average) as well as the oxygen (−0.27). In the gas-phase monomer (Figure 1), C_α acquires a strong negative charge of −1.2, indicative of a carbanion-like character, while C_β acquires a partial positive charge (+0.63). The charges on the O and Li are −0.51 and +0.80, respectively. The presence of two coordinated THF solvent molecules (Figure 4) moderates the charge polarization slightly, yielding $C_\alpha = -0.86$, $C_\beta = +0.47$, O = −0.42, and Li = +0.44. The carbanion character of C_α is present in the gas-phase dimers also (Figure 2), with the charges on the C_α atoms (average of −0.65 over the four C_α's in RR and RS diastereomers) being almost exactly balanced by those on the Li (average of +0.62). These findings are consistent with the tendency of C_α to be highly reactive toward electrophiles.[1−7]

(28) Singh, U. C.; Kollman, P. A. *J. Comput. Chem.* **1984**, *5*, 129; Besler, B. H.; Merz, K. M., Jr.; Kollman, P. A. *J. Comput. Chem.* **1990**, *11*, 431.
(29) Green, D. F.; Tidor, B. *J. Phys. Chem. B* **2003**, *107*, 10261.

Conclusions

Oxiranyllithium is aggregated in the gas phase and in THF solution. In the gas phase, the tetramer predominates, with the *RRRS* diastereomer present in higher concentrations than the *RRRR* or *RRRS*. The dimeric form appears to be favored in solution, with the *RR* isomer is favored over the *RS* by about 2 kcal/mol. The properties of oxiranyllithium appear to be intermediate between a chelated alkyllithium and a lithium carbenoid, with the monomeric structure being more carbenoid-like and the dimer and tetramer more alkllithium-like. Both nucleophilic and carbenoid-like reactions of oxiranyllithiums are known.

Acknowledgment. This work was supported in part by the NSF Grant No. CHE-0139076.

Supporting Information Available: Tables of optimized geometries and energies of all oxiranyllithium structures, and details of the equilibrium calculations presented in Tables 8 and 9. This material is available free of charge via the Internet at http://pubs.acs.org.

JO050887N